REVISTA MATÉRIA V.21 N.03
ISSN 1517-7076 artigo 11726, pp. 569-576, 2016

Structural and morphological analysis of zinc incorporated non-stoichiometric hydroxyapatite nano powders

Hamid Esfahani[1,2], Esmaeil Salahi[1], Ali Tayebifard[1],
Mohammad Reza Rahimipour[1] , Mansour Keyanpour-Rad[1]

[1]Materials and Energy Research Center (MERC), P.O. Box 141554777, Tehran, Iran
[2] Bu-Ali Sina University, Faculty of Technical and Engineering, Materials Science and Engineering Department
Correspond Authors: h-esfahani@merc.ac.ir; e-salahi@merc.ac.ir Tel and Fax: +982636280040-9, POB: 31787-316,
Other Authors Email: a-tayebi@merc.ac.ir; m-rahimi@merc.ac.ir; m.kianpour984@yahoo.com

ABSTRACT

In this study, Zn incorporated non-stoichiometric hydroxyapatite (nHAp) was synthesized via precipitation method and effect of the incorporation of Zn (fraction: 2, 4, 6 and 8 mol-%) on the microstructure of nHAp was studied by XRD, FTIR analysis and SEM-EDS techniques. The formation of nHAp was confirmed by XRD and FTIR those showed that no secondary phase was formed through the Zn incorporation. The SEM studies also revealed that particles were formed in nano-metric size (30-60 nm). It was found that crystallite and particle size of Zn incorporated nHAp gradually decreased up to 6 mol-%, and started to increase while the Zn fraction reached up to the 8 mol-% and hence the morphology of the aggregated products was also changed. It can be concluded that the incorporation of Zn cations cause to form nHAp phase. Furthermore, the nHAp microstructure has deviated from stoichiometric condition by incorporation of more Zn cations.

Keywords: Microstructure; Nanopowder; Non-Stoichiometric Hydroxyapatite; Zn Incorporation

1. INTRODUCTION

Hydroxyapatite (HAp) has been widely used in many biomedical applications such as bone tissue engineering, dental composites, orthopedic implants, antibacterial agents which owes these properties to its chemical and structural similarity with bone minerals and good biocompatibility [1,2]. Recently HAp has found new applications as an absorbent for removing heavy metals from drinkable and waste waters systems [3].

The Ca/P molar ratio of stoichiometric HAp has found to be 1.67. However, the molar ratio of the non-stoichiometric hydroxyapatite (nHAp) varies from 1.5 - 1.67, which is always noticed in the biological conditions because small amounts of anions and cations (e.g. CO_3^{2-} Zn^{2+}) are incorporated in its atomic structure [4-6]. The properties and structure of nHAp have been investigated in some literatures [7,8]. The chemical composition of nHAp is complicated in reality, however the general chemical formula can be presented as formula given in the equation (1) [9].

$$Ca_{10-x}(PO_4)_{6-x}(HPO_4)_x(OH)_{2-x}[0 \le x \le 2] \quad (1)$$

Precipitated or synthetic hydroxyapatite (sHAp) and calcium deficient hydroxyapatite (CDHAp) are also categorized as Non-Stoichiometric Hydroxyapatite due to formation of vacancies or incorporation of foreign cations or anions in the atomic structure of HAp [10,11].

The variety of doping metal elements can be incorporated in HAp, which could change its biological properties, lattice parameters, crystallinity as well as morphology. Incorporation of Zn into the microstructure of HAp has been subjected of recent researches [12,13]. It has been demonstrated that Ca replacement by Zn element in HAp structure causes interesting effects on the properties of this bioceramics. It has been demonstrated that Zn has a stimulatory effect on the bone formation, promotes osteoconductivity and also improves the adsorption ability of proteins by HAp [14].

nHAp powders can be synthesized by several methods, such as hydrolysis, hydrothermal, solid process, sol–gel, spray pyrolysis and wet chemical. The most common and widely technique using for ion incorporated nHAp powder formation is the wet chemical precipitation method [15]. Existence of Zn oxide beside the HAp depends on the procedure of production that good described by Faria *et al.*[16]. It is reported

Corresponding Author: Hamid Esfahani Received on: 09/09/2015 Accepted on: 25/03/2016

10.1590/S1517-707620160003.0055

that Zn oxide could be obtained as a segregate phase in deposition method nor in the ion exchange procedure. The parascholzite phase ($CaZn_2(PO_4)_2.2H_2O$) is formed in composition which contains 20 mol-% or higher amounts of Zn, according to the study performed by F. Miyaji *et al.* [17].

In the present study, wet chemical precipitation method was applied to incorporation of Zn into HAp atomic structure. In order to elucidate the effect of the incorporation of the element into HAp, the detail crystal structure and chemical structure were analyzed by X-Ray diffractometry (XRD), Fourier-Transform Infrared Spectroscopy (FTIR) and Energy Dispersive X-ray Spectroscopy (EDS). To determine the effect of Zn on the particle size and morphology of nHAp aggregates, Scanning Electron Microscopy (SEM) was studied.

2. MATERIALS AND METHODS

2.1 Synthesis of zn-substituted hap

Aqueous phosphate and calcium salts solutions were separately prepared (A) by dissolving of 0.06 mol diammonium hydrogen phosphate [$(NH_4)_2HPO_4$] (Merck, 99% pure, Art No, 1.01207.500) and (B**)** by dissolving of 0.1 mol hydrate calcium acetate [$Ca(CH_3COO)_2.H_2O$] (Merck, 99% pure, Art No. 1.09325.0500) into 50 ml distilled water. The solution (A) was stirred vigorously at 45 ˚C while solution (B) was added dropwise into (A). The pH of the solution was adjusted to 9 by addition of 0.1 M ammonia solution. The precipitating powders were collected and dried at 80 ˚C for 10h. Similar to the above procedure, appropriate amount of dihydrate zinc acetate [$Zn(CH_3COO)_2.2H_2O$] (Merck,extra pure, Art No. 1.08802.0250) was added to solution (B) to synthesis the Zn incorporated HAp powders. The (Ca+Zn)/P molar ratio was kept constant at 1.67 throughout the experiments. In order to investigate the structure of the Zn doped HAp, four different compositions of Zn doped HAp were prepared as a list presented in the Table 1. The amount of Zn was chosen to be 2, 4, 6 and 8 mol-%, representing to Zn/(Zn+Ca) fraction.

Table 1: Composition, chemical analysis, crystallite size and partcle size of synthesised nano-powder

SAMPLE CODE	ZN/(ZN+CA)×100 (MOL %)	EXAMINED (CA+ZN)/P	CRYSTALLITE SIZE (004) (NM)	PARTICLE SIZE (NM)
0ZH	0	1.62	47.5	51
2ZH	2	1.55	37.5	48
4ZH	4	1.53	18.7	42
6ZH	6	1.56	17.1	36
8ZH	8	1.50	37.5	46

2.2 Characterization

The synthesized powders were characterized for their phase contents by X-ray diffraction in the scanning range of 2θ=10-80° (Co-kα1=1.78901 Å, Ni filtered) by Philips PW2273 diffractometer. The developed phases during incorporation process were compared using standard JCPDS files.The crystallite size (t) related to (002) was determined using the equation (2) [18].

$$t = \frac{0.9\lambda}{B\cos\theta_{corr}} \quad (2)$$

Where B is the broadening of the direction line measured at half its maximum intensity (radians) after exerting the silicon correction and λ=1.78901 Å (Co anode tube). Corrections for instrument broadening were made using silicon powder. The corrected 2θ value was calculated by equation (3), where $\Delta 2\theta_{Si}$ is the corrected instrument broadening.

$$2\theta_{corr(sample)} = 2\theta_{obs(sample)} + \Delta 2\theta_{Si} \quad (3)$$

Infrared spectroscopy was performed using a Vector 33-Bruke spectrophotometer. Morphology of the powders was determined using a SEM device (VEGA- TESCAN) equipped by EDS instrument at an accelerating voltage of 15 kV. In order to estimate the Zn fraction EDS analysis was carried out five times at different area of aggregates of powders. To determine the particle size, a drop of suspension of the synthesized powders in water was deposited on a glass plate and sputter-coated with 10 nm of gold and then the images were examined using an Image analyzer.

3. RESULTS AND DISCUSSIONS

3.1 Composition analysis

The EDS spectra of preliminary and Zn incorporated HAp powders are presented in Fig.1. As can be noticed, the spectra of the powders have been overlapped except in the region of 0.8 to 1.2 keV shown by a circle in the upper right side of Fig.1. The X-ray energy dispersed spectrum related to the Zn-Lα is intensified by increasing amount of Zn. In accordance to the data, the presence of Ca, Zn and P are confirmed by this analysis in all the samples. The (Ca+Zn)/P molar ratio of the synthesized powders was calculated by obtained data from EDS analysis as amounts summarized in Table 1. The relative deviation of 5% in the (Ca+Zn)/P molar ratio is generally considered to be acceptable [7].

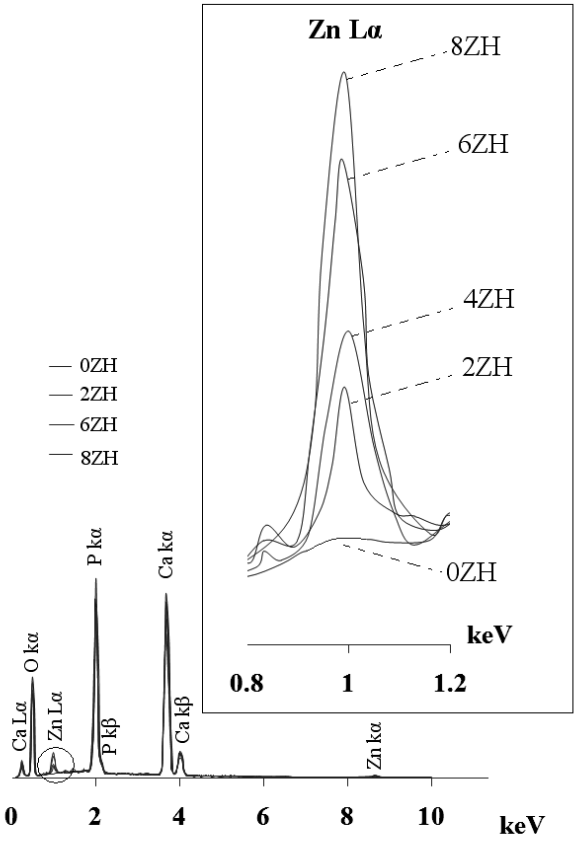

Figure 1: Spectra of undoped and Zn incorporated HAp

3.2 Phase analysis

The X-ray diffraction patterns of the powders are plotted in Fig.2. The XRD pattern of the undoped powder (0ZH) has both similarities and differences compared to the pure hydroxyapatite based on standard card. It can be hypothesis that non-stoichiometric hydroxyapatite was formed even not any Zn cations incorporated into HAp. Although diffracted planes were coincidence to stoichiometric HAp planes, but high crystalline HAp were not obtained. Our results show that CDHAp an aspect of nHAp has been achieved. It is in good agreement with the literatures findings [19].

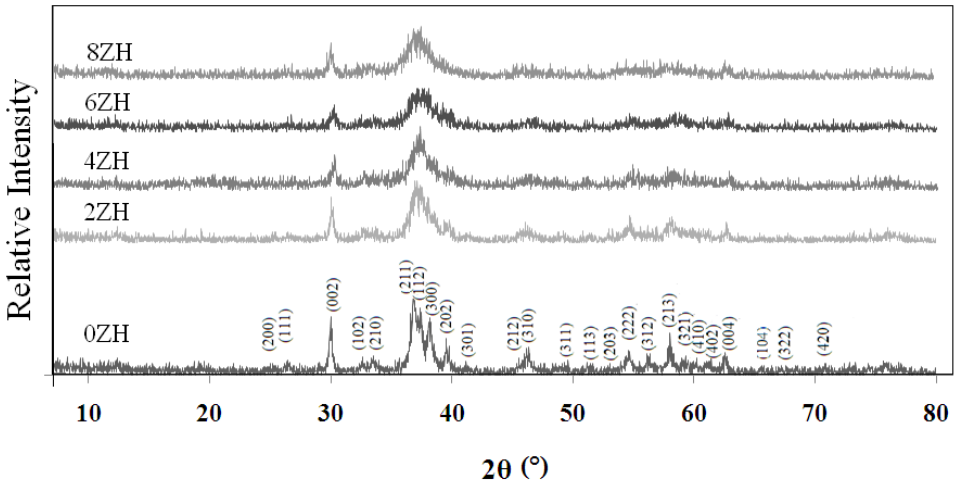

Figure 2: XRD patterns of pure and Zn incorporated HAp

Variation of Zn fraction has effect on the X-ray diffraction pattern of the nHAp as obviously illustrated in Fig.2. The XRD pattern of the Zn doped powders indicates that it was only formed as a single phase compound and the other Zn compounds such as ZnO or $CaZn_2(PO_4)_2.2H_2O$ were not formed. It can be seen that crystalline pattern of 0ZH decreased by increasing the Zn content up to 6 mol-% and then started to increase slowly. Furthermore, the planes (211), (112), (300) and (202) merged together forming a broad peak. The broad XRD pattern of the Zn content powders indicates the nano-crystalline nature of the particles which is consistent with the results listed in Table 1.

3.3 Ftir spectroscopy

To avoid potential incorporation of nitrate or chloride ions in the apatite structure [17], the acetate salts of Ca and Zn were used instead of nitrate or chloride precursor. Fig. 3 shows the FTIR spectra of the synthetic powders. The most characteristic chemical groups appeared in the FTIR spectrum are PO_4^{3-} and OH^- as well as HPO_4^{2-} indicating the formation of nHAp with formula as given in equation (1).

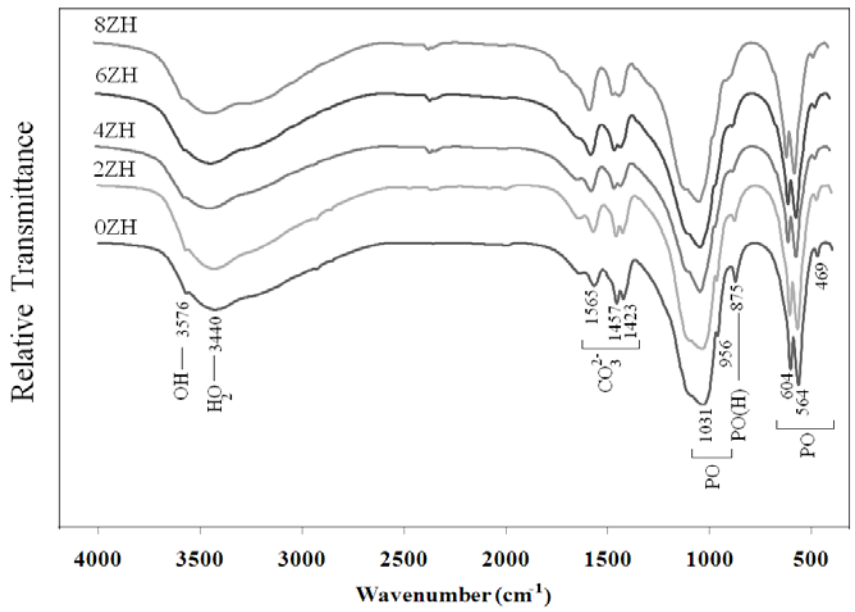

Figure 3: FTIR Spectra of undoped and Zn incorporated HAp

Theoretically, there should be four vibrations modes (ν_1- ν_4) for the phosphate ions [20]. A low intensity band at 469 cm^{-1} and the double bands at 564 and 604 cm^{-1} belong to bending vibrations of P-O (υ_2 and υ_4 respectively). The bands at 956 and 1031cm^{-1} are assigned to fundamental frequencies of symmetric (υ_1) and anti-symmetric (υ_3) stretching vibrations of P-O band, respectively. A low intensity band at 875 cm^{-1} is assigned to the stretching vibrations of P-O(H) in HPO_4^{2-} group. Although P-O(H) band can be assigned to the starting material (diammonium hydrogen phosphate), but existence of HPO_4^{2-} group is characterized as CDHAp. Uncontrollable substitution of the PO groups by PO(H) in 0ZH sample causes a decrease in Ca/P molar ratio from the theoretical ratio 1.67. This is because the Ca and OH vacancies were created to satisfy the electrical charge neutrality [7].

The broad band at 3440 cm^{-1} belongs to physically adsorbed water. The narrow band at 3576 cm^{1} and also the band at 630 cm^{-1} appeared as a shoulder, are assigned to structural OH. Carbon dioxide can be dissolved in solution as a common contaminant from the atmosphere during the precipitation process and then incorporates in the amorphous complex followed by penetration into HAp and thus tending to form a deficient form of HAp. In this case type A is considered when the carbonate replaces at the hydroxyl site and type B when replacement occurs at the phosphate site. Therefore, the bands at 1423-1565 cm^{-1} are assigned to CO_3^{2-} group. According to FTIR spectra, it can be noticed that the nHAp with low crystallinity has been formed, which agrees to the XRD data.

The FTIR spectrum of the 2 mol-% Zn doped HAp has also indicated that Zn helps to stabilize the CDHAp phase (Fig.3). As can be seen, the FTIR spectra of the 4, 6 and 8 mol-% Zn are not drastically different from the undoped HAp, except for the transmitted intensity of P-O(H) band at 875 cm^{-1}, which has been decreased by increasing the Zn fraction. By assumption of general formula of inserted Zn cation in HAp [21]; $Ca_{10}Zn_x(PO_4)_6(OH)_{2-2x}O_{2x}$ the decrease of HPO_4^{2-} group would then be elucidated. The FTIR results showed that the P-O(H) band at 875 cm^{-1} decreased up to the 6 mol-% and started to increase in the 8 mol-% Zn fraction. As can be seen in the FTIR spectra, by increasing the Zn fraction, the shape of P-O bands was changed. These changes suggest that the crystallinity of the HAp decreased by increasing Zn fraction [19]. This is in agreement with the results obtained from the XRD pattern. Moreover, the narrow band of structural OH^- was remained in the spectra and the broad band of the absorbed water was not disappeared.

3.4 Particle size and morphology

The crystallite size related to (002) plane are calculated from Scherrer equation (see Table 1), and the average size of the synthesized particles are showed in Fig 4. The results indicated that the size of the crystallites and also particles harmoniously reduced by increasing Zn fraction up to the 6 mol-% and then started to grow. E. Fujii *et al.* [14], reported similar behavior in their study on Zn incorporation into HAp. The particle size was distributed over a rather narrow range in our study. In contrast, the diameters of the grains were distributed over a wide range as studied by T.J. Webster *et al*. [22]. Regardless of inconsistent results in the literatures for particle size, the SEM images and crystallite estimation indicated that the crystallinity of the HAp decreased by increasing of Zn fraction up to the 6 mol-% and then started to increase in the 8 mol-%, which is in agreement with the results obtained from XRD and FTIR studies. As listed in Table.1, the minimum average particles size and the crystallite size related to the 6ZH sample are 36 and 17.1nm, respectively.

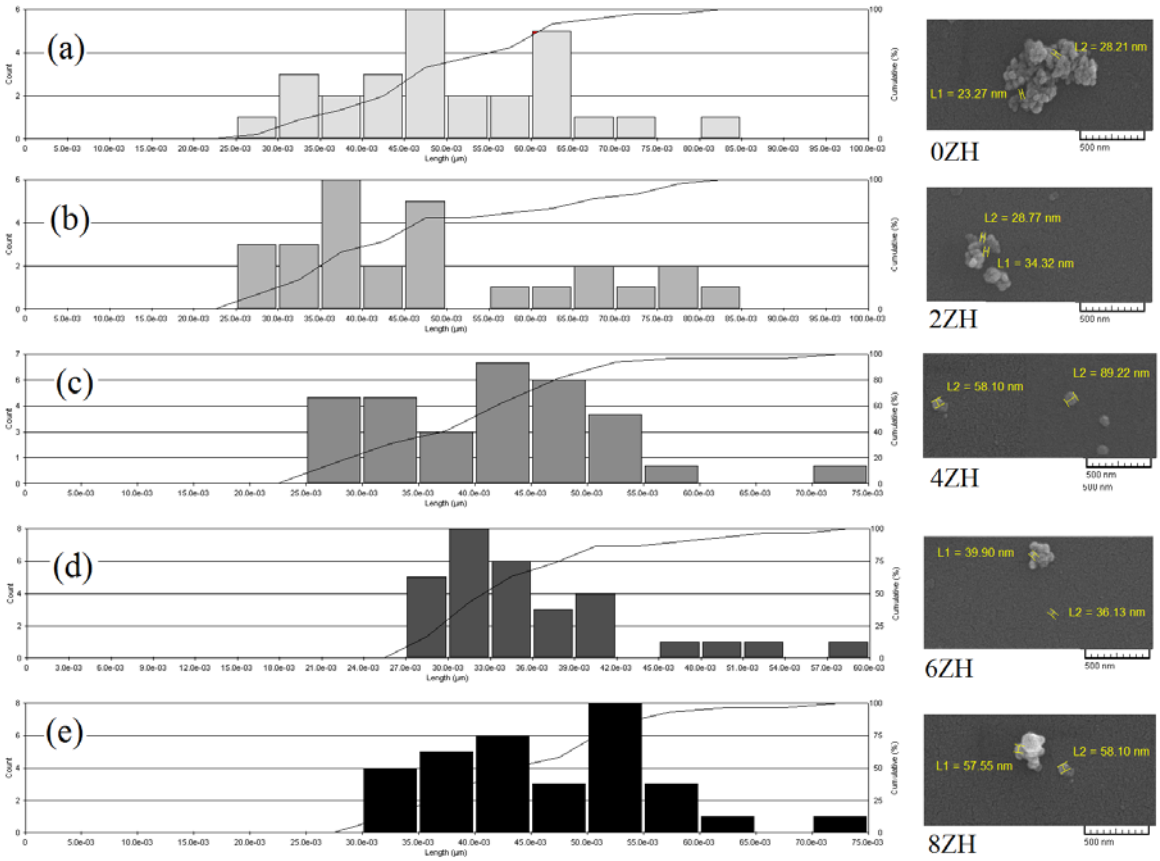

Figure 4: Distribution size curve and SEM of (a) 0ZH, (b) 2ZH, (c) 4ZH, (d) 6ZH, (e) 8ZH nanoparticles

Furthermore, the morphology of 0ZH powder was changed by incorporation of the Zn particles as shown in Fig.5(a-e). It can be observed that the 0ZH powder sample has a cauliflower-shape which could be changed to an irregular rough-shape by increasing the Zn fraction up to the 6 mol-% and not any tinsel-shape can be seen on the 6ZH aggregates. It could also be seen that the tiny tinsel-shape was formed on the 8ZH aggregates. It can be argued that this behavior is due to crystallinity of the synthesized powder.

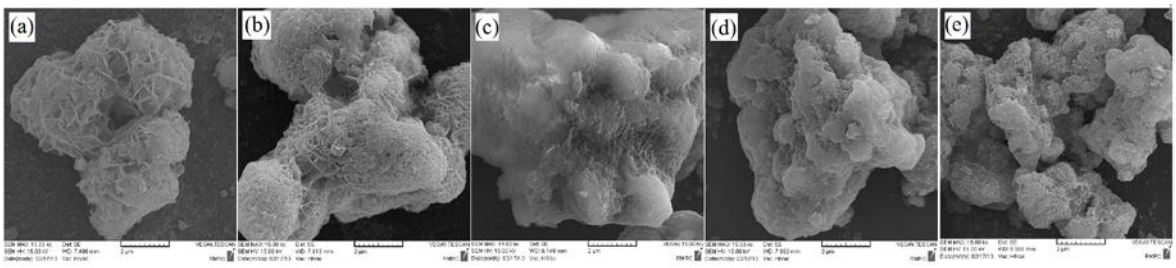

Figure 5: SEM micrographs of aggregates of products (a) undoped HAp, (b) 2ZH, (c) 4ZH, (d) 6ZH, (e) 8ZH nano powders

4. CONCLUSIONS

In this study, Zn incorporated non-stoichiometric hydroxyapatite was synthesized via precipitation method and the effect of Zn incorporation on the atomic structure of hydroxyapatite was studied. Intensifying Lα- Zn peak in EDS spectra of the synthesized powders revealed the incorporation of Zn^{2+} in HAp framework by increasing the Zn fraction. At the same time it was confirmed that (Ca+Zn)/P ratio revealed the formation of a nHAp. The XRD pattern as well as FTIR spectra showed that single CDHAp phase was formed as a nHAp.

The crystallite and particle size of Zn incorporated HAp decreased by increasing the Zn fraction up to the 6 mol-% and then started to grow by increasing the Zn fraction up to 8 mol-% due to change of

crystallinity of synthesized powder which is in agreement with XRD and FTIR results. Similarly, the morphology of the aggregated products was changed from cauliflower to irregular rough shape due to change of crystallinity of products.

5. BIBLIOGRAPHY

[1] KALITA S. J., BHARDWAJ A., BHATT H. A. "Nanocrystalline calcium phosphate ceramics in biomedical engineering", *J. Materials Science Engineering* C.v. 27, pp. 441–449, 2007.

[2] CHEN L., MCCRATE, J.M., JAMES C., *et al.*, "The role of surface charge on the uptake and biocompatibility of hydroxyapatite nanoparticles with osteoblast cells", *J. Nano technology*, v.22, pp. 105708, 2011.

[3] MOBASHERPOUR I., SALAHI E., PAZOUK M., "Comparative of the removal of Pb^{2+}, Cd^{2+} and Ni^{2+} by nano crystallite hydroxyapatite from aqueous solutions: Adsorption isotherm study", *Arabian Journal of Chemistry*, v.5, n.4, pp. 439-446, 2012.

[4] FU OU, S., CHIOU, S.Y., LIANG OU, K., "Phase transformation on hydroxyapatite decomposition", *Ceramic International*, v.39, n.4, pp. 3809-3816, 2013.

[5] KANNAN, S., VENTURA, J.M.G., FERREIRA, J.M.F., "Synthesis and thermal stability of potassium substituted hydroxyapatites and hydroxyapatite/β-tricalciumphosphate mixtures", *Ceramic International*, v. 33, n. 8, pp. 1489-1494, 2007.

[6] EVIS Z., YILMAZ B., USTA M., AKTUG S.L."X-ray investigation of sintered cadmium doped hydroxyapatites", *Ceramic International*, v. 39, n. 3, pp. 2359-2363, 2013.

[7] MOGHIMIAN, P., NAJAFI, A., AFSHAR, S., *et al*., "Effect of low temperature on formation mechanism of calcium phosphate nano powder via precipitation method", *Advanced Powder Technology*,. v.23, n. 6, pp. 744-751, 2012.

[8] KURIAKOSE, T.A., KALKURA, S.N., PALANICHAMY, M., *et al*., "Synthesis of stoichiometric nano crystalline hydroxyapatite by ethanol-based sol–gel technique at low temperature", *Journal of Crystal Growth*, v. 263, n.1–4, pp. 517-523, 2004.

[9] KANNAN, S., VENTURA, J.M., FERREIRA, J.M.F. "Aqueous precipitation method for the formation of Mg-stabilized β-tricalcium phosphate: An X-ray diffraction study", *Ceramic International*, v. 33, n. 4, pp. 637-641, 2007.

[10] MATSUNAGA, K., MURATA, H., MIZOGUCHI, T., *et al*., "Mechanism of incorporation of zinc into hydroxyapatite", *Acta Biomaterialia*, v. 6, pp. 2289–2293, 2010.

[11] KUMAR , G. S., THAMIZHAVEL, A., YOKOGAWA, Y., *et al*., "Synthesis, characterization and in vitro studies of zinc and carbonate co-substituted nano-hydroxyapatite for biomedical applications", *Materials Chemistry and Physics*, v.134, pp. 1127-1135, 2012.

[12] UYSAL, I., SEVERCAN, F., EVIS, Z. "Characterization by Fourier transform infrared spectroscopy of hydroxyapatite co-doped with zinc and fluoride", *Ceramic International*, v. 39, n. 7, pp. 7727-7733, 2013.

[13] KAWABATA, K., YAMAMOTO, T., KITADA, A., "Substitution mechanism of Zn ions in b-tricalcium phosphate", *Physica B*, v. 406, pp. 890–894, 2011.

[14] FUJII, E., OHKUBO, M., TSURU, K., *et al.*, "Selective protein adsorption property and characterization of nano-crystalline zinc-containing hydroxyapatite", *Acta Biomaterialia*, v. 2, n. 1, pp. 69-74, 2006.

[15] CACCIOTTI, I., BIANCO, A., "High thermally stable Mg-substituted tricalcium hosphate via precipitation", *Ceramic International*, v. 37, n. 1, pp. 127-137, 2011.

[16] FARIA, R. M.B., CESAR, D. V., SALIM, V. M.M. "Surface reactivity of zinc-modified hydroxyapatite", *Catalysis Today*, v.133–135, pp. 168–173, 2008.

[17] MIYAJI, F., KONO, Y., SUYAMA, Y., "Formation and structure of zinc-substituted calcium hydroxyapatite", *Materials Research Bulletin*, v. 40, pp. 209–220, 2005.

[18] KNOWLES, J.C., CALLCUT, S., GEORGIOU, G. "Characterization of the rheological properties and zeta potential of a range of hydroxyapatite powders", *Biomaterials*, v. 21, pp. 1387-1392, 2000.

[19] DOROZHKIN, S. V., "Amorphous calcium (ortho) phosphates", *Acta Biomaterialia*, v. 6, pp. 4457–4475, 2010.

[20] ESFAHANI, H., DABIR, F., TAHERI, M., *et al*., "Sol–gel derived hydroxyapatite coating onTiB_2/TiB/Ti substrate", *Surface Engineering*, v. 8, n. 7, pp. 526- 531, 2012.

[21] NEDELEC, J.M., RENAUDIN, G., GOMES, S., "On the effect of temperature on the insertion of zinc into hydroxyapatite", *Acta Biomaterialia*, v. 8, 1180–1189, 2012.

[22] WEBSTER, T. J., MASSA-SCHLUETER, E.A., SMITH, J. L., Slamovich E. B., "Osteoblast response to hydroxyapatite doped with divalent and trivalent cations", *Biomaterials*, v. 25, pp. 2111–2, 2004.